Electronic Supplementary Material (ESI) for Journal of Materials Chemistry A.

Tunable Pseudocapacitance Storage of MXene by Cation Pillaring for High-Performance Sodium Ion Capacitors

Jianmin Luo,[a,b] Cong Fang,[a] Chengbin Jin,[a] Huadong Yuan,[a] Ouwei Sheng,[a] Ruyi Fang,[a] Wenkui Zhang,[a] Hui Huang,[a] Yongping Gan,[a] Yang Xia,[a] Chu Liang,[a] Jun Zhang,[a] Weiyang Li,[b,*] and Xinyong Tao[a,*]

[a] *College of Materials Science and Engineering, Zhejiang University of Technology, Hangzhou 310014, People's Republic of China;* [b] *Thayer School of Engineering, Dartmouth College, Hanover, New Hampshire 03755, United States*

**Address correspondence to, Weiyang.Li@dartmouth.edu* (W. Li), *tao@zjut.edu.cn* (X. Tao)

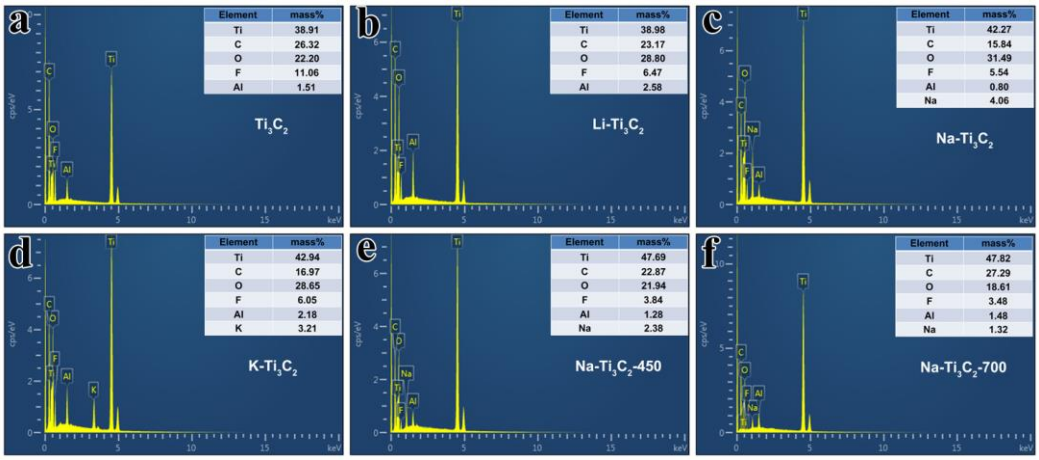

Fig. S1 Energy dispersive spectroscopy of (a) Ti_3C_2, (b) Li-Ti_3C_2, (c) Na-Ti_3C_2, (d) K-Ti_3C_2, (e) Na-Ti_3C_2-450, (f) Na-Ti_3C_2-700.

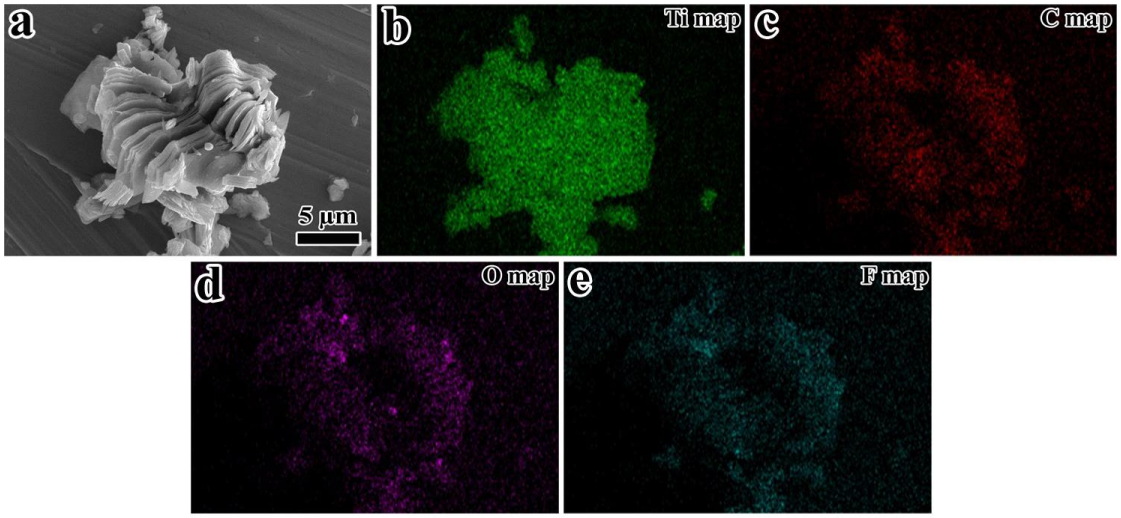

Fig. S2a (a-e) SEM image of Ti_3C_2 and elemental mapping of Ti, C, O and F, which confirm the homogeneously distribution of –OH and –F groups in all MXene sheets.

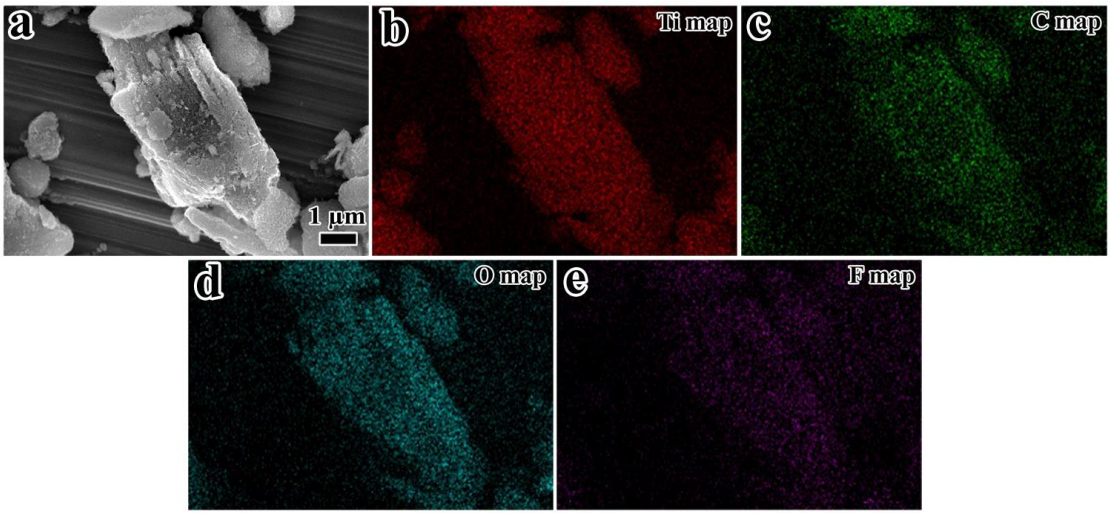

Fig. S2b (a-e) SEM image of Li-Ti_3C_2 and elemental mapping of Ti, C, O and F. After Li^+ pillaring, the –F groups was replaced by –OH due to the decrease intensity of the F signal and the increase intensity of the O signal compared with those in Ti_3C_2, while the signal of Li can't be detected by EDS.

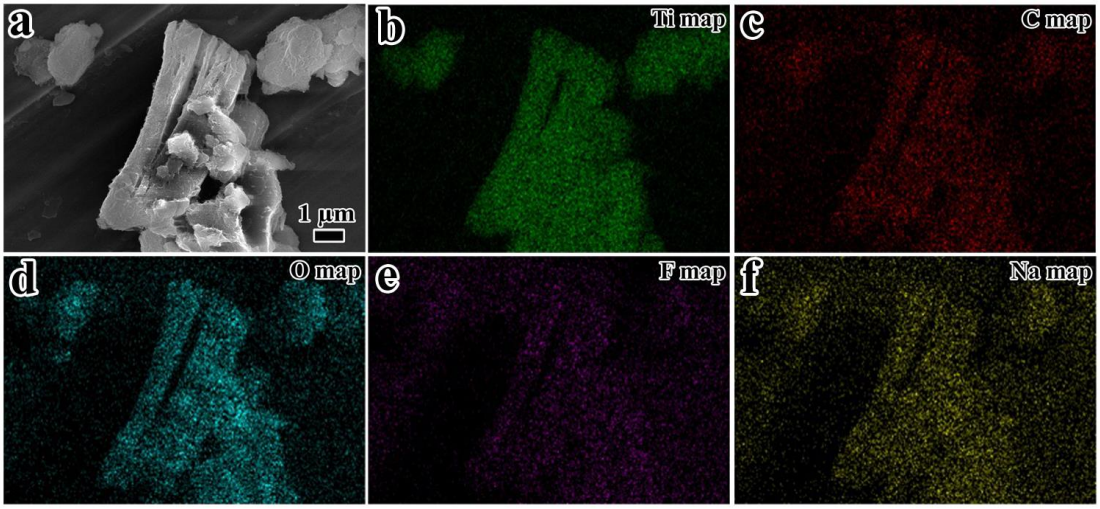

Fig. S2c (a-f) SEM image of Na-Ti_3C_2 and elemental mapping of Ti, C, O, F, and Na, which confirm the homogeneous distribution of Na in all MXene sheets. After Na^+ pillaring, the –F groups was replaced by –OH due to the decrease intensity of the F signal and the increase intensity of the O signal compared with those in Ti_3C_2.

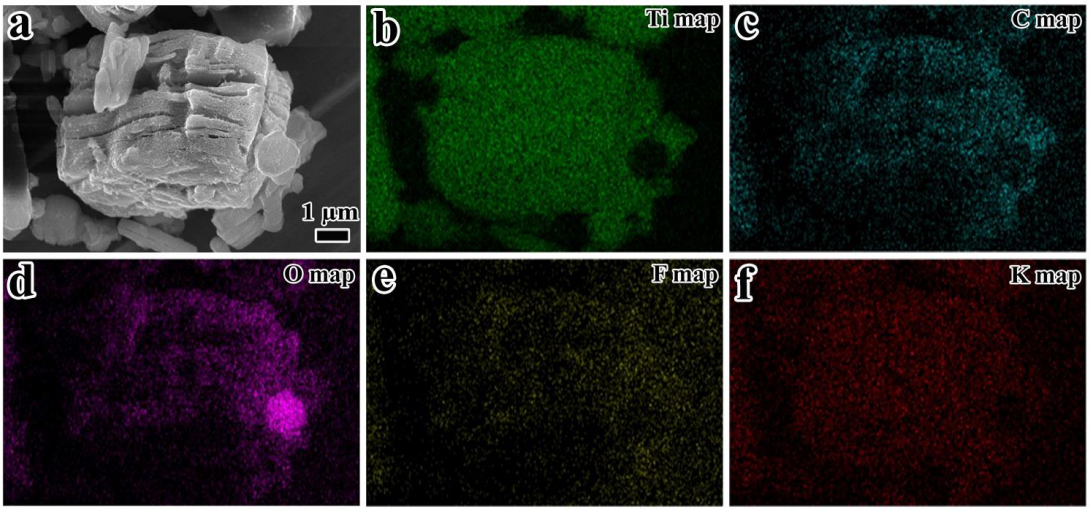

Fig. S2d (a-f) SEM image of K-Ti_3C_2 and elemental mapping of Ti, C, O, F, and K, which confirms the homogeneous distribution of K in all MXene sheets. After K^+ pillaring, the –F groups was replaced by –OH due to the decrease intensity of the F signal and the increase intensity of the O signal compared with those in Ti_3C_2.

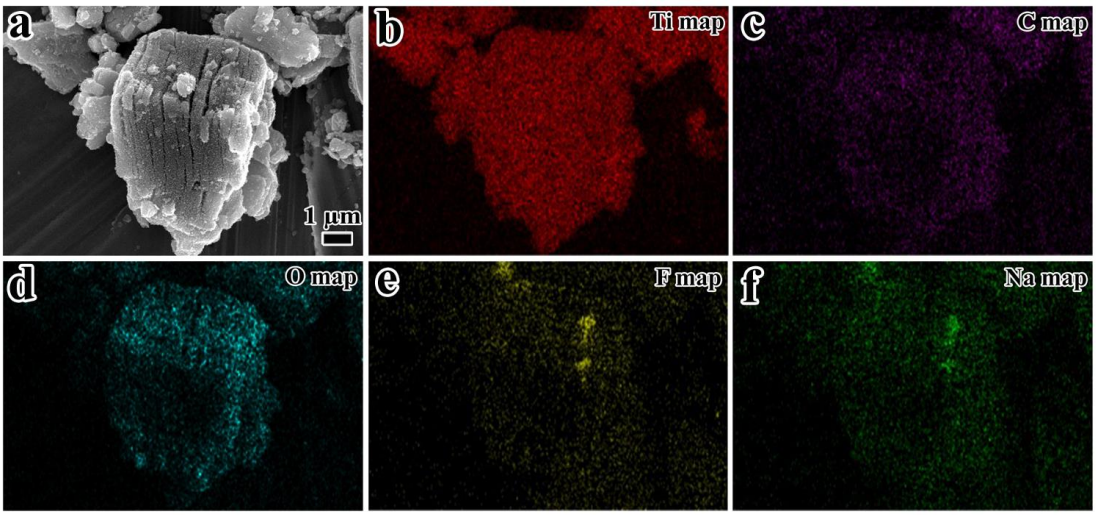

Fig. S2e (a-f) SEM image of Na-Ti_3C_2-450 and elemental mapping of Ti, C, O, F, and Na, which confirms the homogeneous distribution of Na in all MXene sheets after calcinations at 450 ºC. The O signal decreased compared with Na-Ti_3C_2.

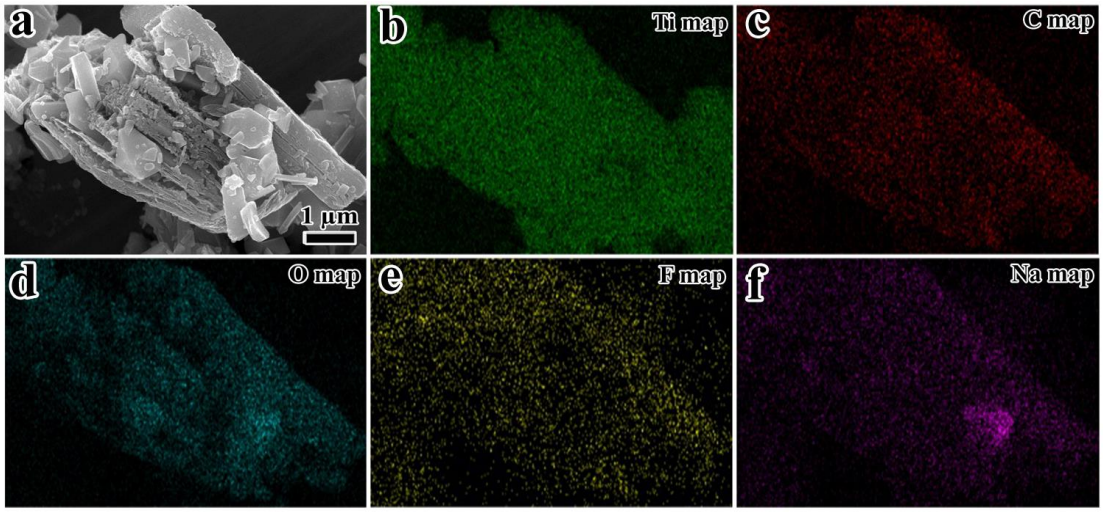

Fig. S2f (a-f) SEM image of Na-Ti_3C_2-700 and elemental mapping of Ti, C, O, F, and Na, which confirms the homogeneous distribution further of Na in all MXene sheets after calcinations at 700 ºC. The O signal decreased further compared with Na-Ti_3C_2-450.

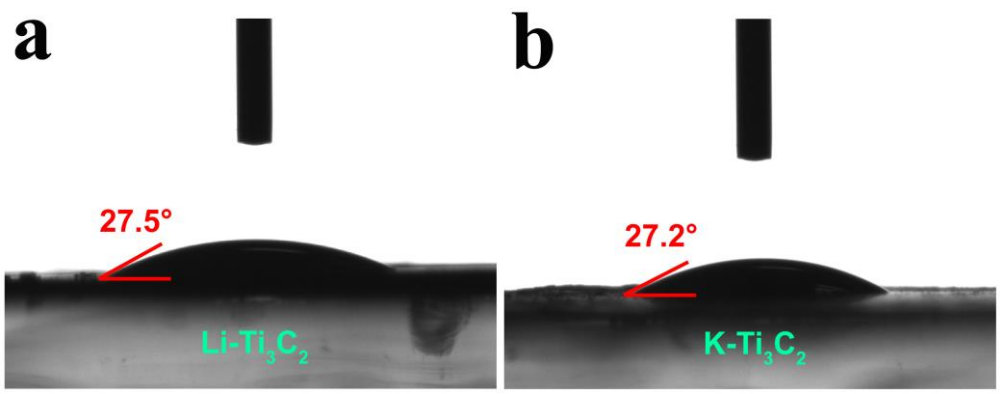

Fig. S3 (a, b) Surface wetting of the water droplet on the Li-Ti_3C_2, K-Ti_3C_2.

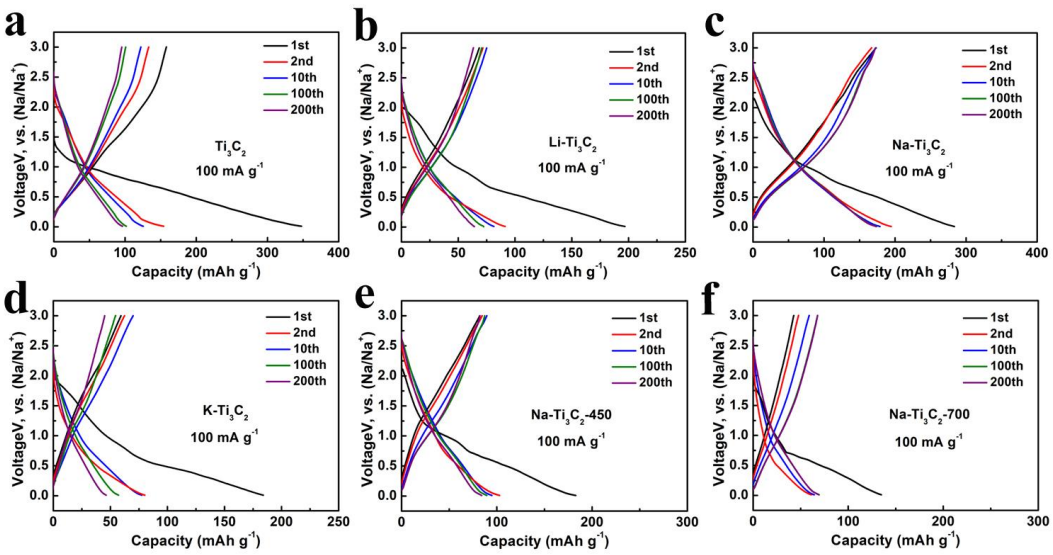

Fig. S4 The galvanostatic charge/discharge profiles of (a) Ti_3C_2, (b) Li-Ti_3C_2, (c) Na-Ti_3C_2, (d) K-Ti_3C_2, (e) Na-Ti_3C_2-450, and (f) Na-Ti_3C_2-700 at a current density of 0.1 A g^{-1}.

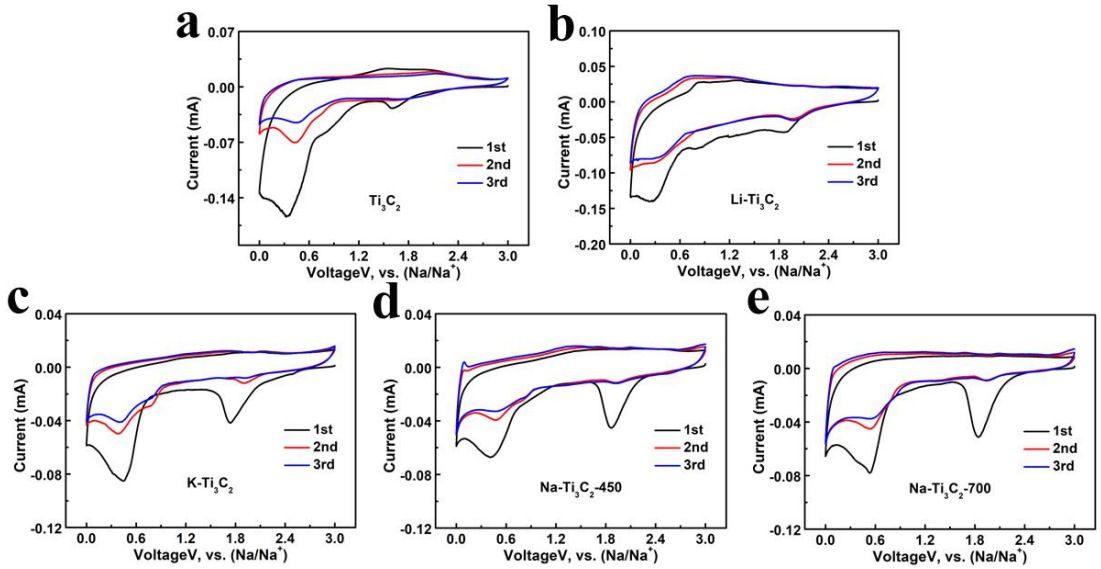

Fig. S5 CV curves of (a) Ti_3C_2, (b) Li-Ti_3C_2, (c) K-Ti_3C_2, (d) Na-Ti_3C_2-450, and (e) Na-Ti_3C_2-700 at 0.1 mV s^{-1}.

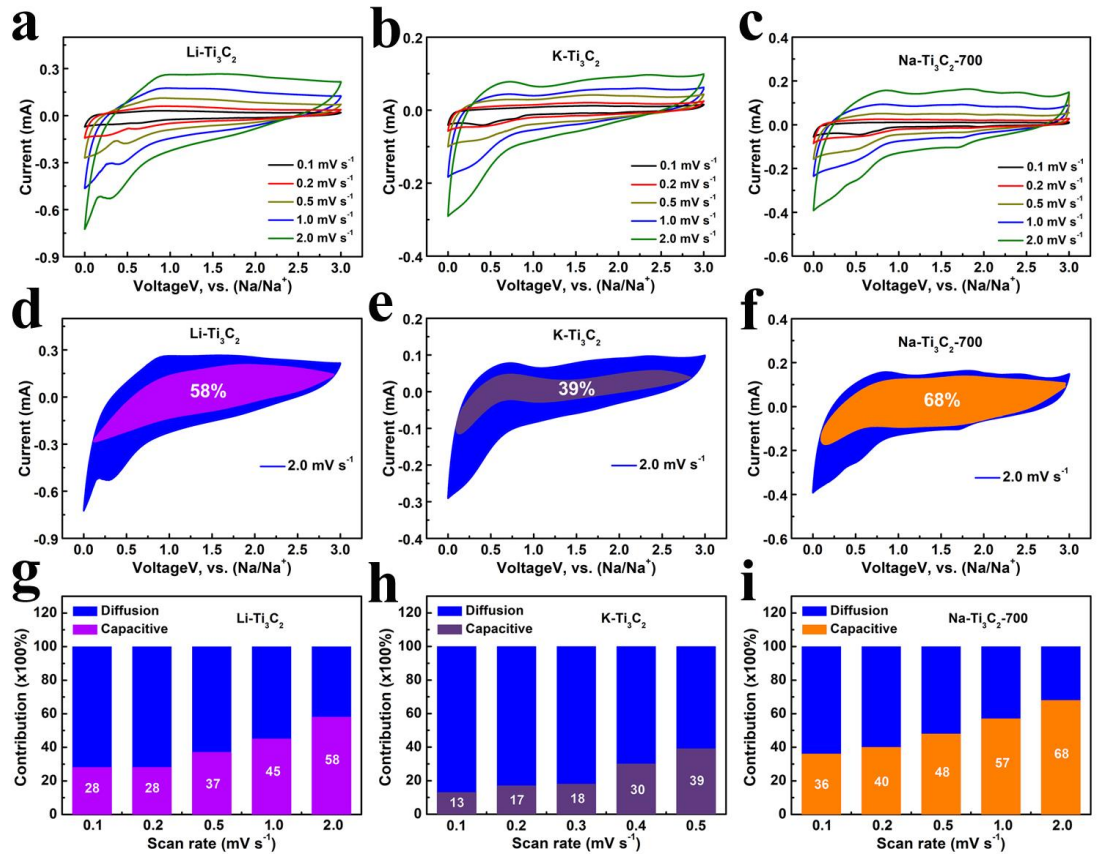

Fig. S6 (a-c) CV curves of Li-Ti_3C_2, K-Ti_3C_2, and Na-Ti_3C_2-700 electrodes at different scan rates. (d-f) Capacitive and diffusion currents (blue) contributed to charge storage of Li-Ti_3C_2, K-Ti_3C_2, and Na-Ti_3C_2-700 at a scan rate of 2.0 mV s^{-1}. (g-i) The percentage of capacitance contribution of Li-Ti_3C_2, K-Ti_3C_2, and Na-Ti_3C_2-700 at different scan rates (0.1-2.0 mV s^{-1}).

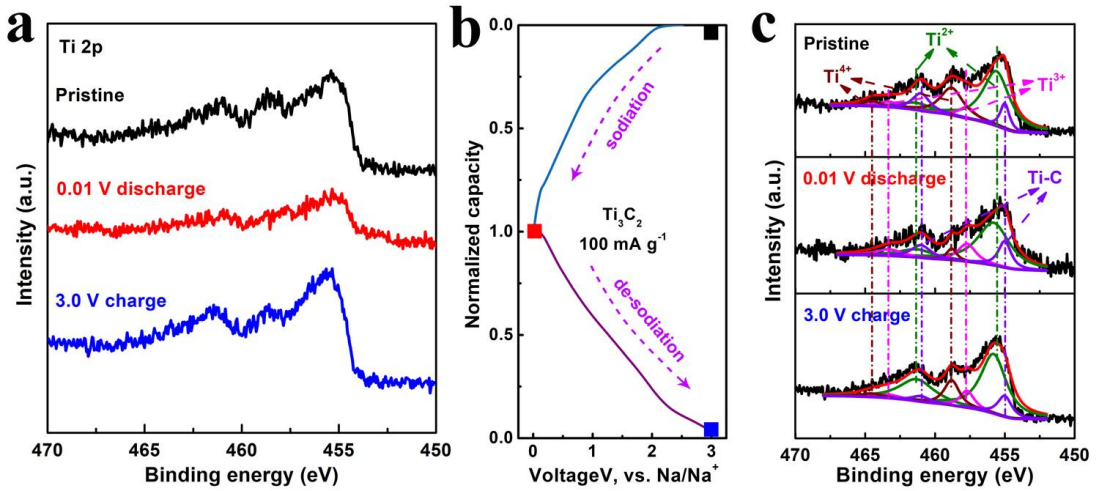

Fig. S7 Ex situ XPS studies for the Ti_3C_2. (a) The ex situ XPS spectra of the Ti 2p peaks to survey the changes in valence states of Ti during the sodiation and de-sodiation processes about Ti_3C_2. (b) Voltage profiles of Ti_3C_2 in different states of sodiation/desodiation at which the samples were taken for ex situ XPS test. (c) The Ti 2p peaks of Ti_3C_2 samples at pristine state, 0.01 V discharge state, 3.0 V charge state.

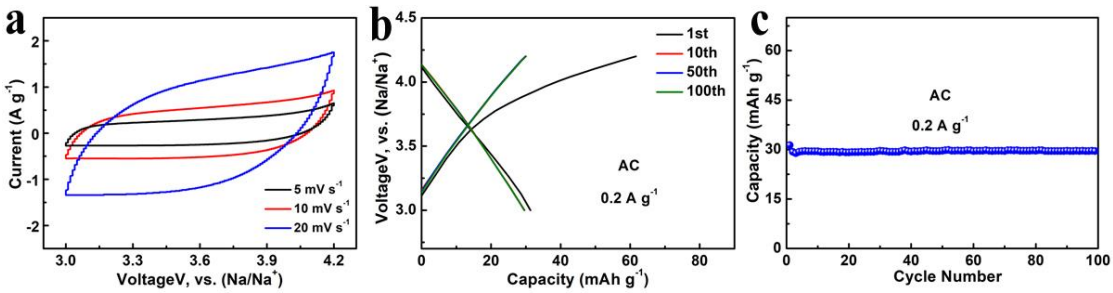

Fig. S8 (a) The CV Curves of AC at different scan rates between 3.0-4.2V. (b) The charge-discharge curves of AC at 0.2 A g^{-1} between 3.0-4.2V. (c) The cycling performance of AC at 0.2 A g^{-1} between 3.0-4.2V.